

Technical Notes

TECHNICAL NOTES are short manuscripts describing new developments or important results of a preliminary nature. These Notes cannot exceed 6 manuscript pages and 3 figures; a page of text may be substituted for a figure and vice versa. After informal review by the editors, they may be published within a few months of the date of receipt. Style requirements are the same as for regular contributions (see inside back cover).

Combined LDV and Rayleigh Measurements in a Complex Turbulent Mixing Flow

W. A. de Groot,* R. E. Walterick,* and
J. I. Jagoda†
Georgia Institute of Technology,
Atlanta, Georgia

Introduction

SOLID fueled ramjets (SFRJ), as other ramjets, require a flame-anchoring region at the head of the combustion chamber. Here the flow must be turbulent to facilitate mixing of fuel and air and have a velocity lower than the flame propagation speed of the mixture. Such a flow exists in the recirculation zone behind a backward-facing step. The work in this laboratory investigates the complex turbulent flowfield resulting from a fuel injected through a porous plate (to simulate the pyrolysis of a solid fuel) into the recirculation region behind such a backward-facing step. The part of the study reported here deals with a cold flow simulation of this process. Combined laser Doppler velocimetry (LDV) and molecular Rayleigh scattering were used to determine the flow velocity and bleed gas concentration distributions. In addition, the correlation between the velocity and concentration fluctuations resulted in information about turbulent mass transport in the flowfield. The results of these measurements were compared with the predictions obtained using a modified $k-\epsilon$ model, reported elsewhere.^{1,2}

Experimental Work

The tunnel used in this investigation has previously been described in detail.³ Briefly, air drawn from the laboratory passes over a backward-facing step and establishes a recirculation zone. The injectant gas is bled into the recirculation zone through a porous floor behind the step. In the present study, a CO₂-air mixture was used as the bleed gas since the Rayleigh scattering cross section of CO₂ is 2.4 times that of air.⁴ The CO₂ was bled from a large tank filled to 100 psi with compressed CO₂ gas. The long line from the tank to the facility assured that the CO₂ entered the test section close to room temperature. In order to conserve bleed gas, injection was limited to a region between two and eight step heights behind the step. Optical access was provided through antireflection-coated glass side windows.

Velocities and bleed gas concentrations were measured simultaneously using a combined LDV-Rayleigh scattering system. The LDV is a TSI, two-component system with Bragg cells using a 5-W argon ion laser. The Rayleigh system used the

LDV laser as a light source. Scattered light is focused by an F/10 lens through an interference filter onto a 500 μm -pinhole placed in front of a photomultiplier (PM) (HAMAMATSU R269) selected for low shot noise. The photomultiplier output is amplified, passed through an A/D converter (Preston), and stored along with the LDV data in the computer.

The 514.5-nm beam of the laser was used to measure the vertical velocities as well as the Rayleigh scattering since its orientation with respect to the tunnel minimized the background scatter entering the photomultiplier. The entire optical system was mounted on a remotely controlled actuator and inclined through a small angle to the horizontal. This allowed measurements down to 0.1 step heights above the floor. Closer to the porous plate, reflections from the plate interfered with the Rayleigh measurements.

While the LDV needs seed particles in the flow, seeding interferes with the concentration measurements, since the scattering cross sections of particles are orders of magnitude larger than those of molecules. Only dust in the laboratory air, therefore, was used in these tests. The injected flow could not be seeded since particles would plug the porous plate. It will be shown that this did not cause a detectable concentration bias, even close to the porous plate.

The combined LDV-Rayleigh measurements reported here had to be carried out under more adverse conditions than those by other workers.^{5,6} Because of the size of the tunnel, the LDV measurements had to be carried out in backscatter. The optical axis of the Rayleigh detection system had to be placed at an angle of 27.5 deg to the incident beam rather than at 90 deg, which would have minimized the Mie scattering from seed particles. The small aspect ratio of the tunnel, necessary to prevent wall effects from affecting the two-dimensionality of the flow, limited the F number of the Rayleigh optics to 10.

Data Acquisition and Analysis

For this part of the study, only vertical velocities were recorded. Velocity signals were processed into probability density functions (pdf) from which mean and rms velocities were calculated. The output from the Rayleigh PM was stored either as pure Rayleigh or LDV-triggered Rayleigh measurements. For the pure Rayleigh measurements, the PM output was sampled at a rate of 125,000 data/s. Thirty-two thousand Rayleigh data points were collected at each location and processed into pdf's, from which mean and rms concentrations were determined. In the second technique, the Rayleigh signals were measured simultaneously with those from the LDV. Since the arrival times of the seed particles for the velocity measurements were random, Rayleigh scattering data had to be acquired continuously and matched with the velocity data from the LDV counters. For this purpose, the memory of the computer was divided into three buffers. Newly arriving Rayleigh data were stored in one 32 K buffer while the velocity data were stored in a second 32 K buffer until the Rayleigh buffer was filled. The LDV buffer then was searched for validated data points, which were matched with the corresponding Rayleigh values. Twenty Rayleigh points at 8- μs intervals were collected before and after each validated velocity measurement and averaged and stored along with their velocity values in the third memory buffer. The LDV and Rayleigh buffers then were overwritten with new data. The low seed rate required for successful Rayleigh measurements resulted in a typical data rate of 10–20 data/s. Since a full tank load of CO₂ only provided a 30-min run time, only 1000 combined velocity-concentration data pairs were mea-

Presented as Paper 87-1328 at the AIAA 19th Fluid Dynamics, Plasma Dynamics and Lasers Conference, Honolulu, HI, June 8–10, 1987; received Sept. 8, 1987; revision received March 11, 1988. Copyright © American Institute of Aeronautics and Astronautics, Inc., 1987. All rights reserved.

*Research Engineer, School of Aerospace Engineering. Member AIAA.

†Associate Professor, School of Aerospace Engineering. Member AIAA.

sured at each position. Rayleigh signals above a threshold voltage, selected to discard signals caused by scattering from particles in the test volume while still accepting those from pure CO_2 , were rejected.

Both continuous and LDV-triggered concentration measurements were carried out at each location. In addition, pure LDV measurements were made, bleeding air and seeding the main flow with titanium dioxide particles. Because of the heavier seeding, it was possible to obtain 10,000 velocity points per location, which were compared with the results of the 1000-LDV data from the combined measurements. Furthermore, comparison of the continuous and LDV-triggered concentration measurements permitted a check for possible concentration bias toward higher air concentrations when the Rayleigh signal was only accepted as a seed particle passed through the test volume. Such bias could have been possible since the bleed gas could not be seeded.

In order to obtain quasisimultaneous measurements of velocity and concentration, the noise due to the background scattering, the polydispersion of dust particles, and the short run times had to be removed from the molecular scattering signals. To this end, a complex data reduction scheme was developed.

A simplified data reduction scheme based on the assumption that particle-generated noise was independent of local CO_2 concentration resulted in CO_2 concentration profiles, which were previously reported.³ However, a close inspection of the shape of the concentration pdf's revealed a small change in the contribution to the pdf's by dust particles, depending on the local concentrations of the bleed gas. This caused minor changes in the profiles of the mean concentrations but introduced an unacceptable error in the velocity-concentration covariances, which are far more sensitive to the quality of the data. A more sophisticated data reduction technique, therefore, was developed. Here, the dependence of the contributions of the particle noise to the measured pdf's upon the concentration of injectant gas at each point was accounted for. In addition, the actual pdf's of the electronic and particle-generated noise rather than their means were subtracted out. This paper reports the mean CO_2 concentrations obtained using this improved technique. Furthermore, the velocity-concentration covariances that could not be obtained from the measurements using the simplified data reduction scheme were calculated using the velocity weighted pdf's in the new data reduction technique and are presented. The mathematical details of this novel deconvolution technique have been published in *Combustion and Flame*⁷ and, therefore, will not be repeated here.

Results and Discussion

Local velocity, bleed gas concentration, and simultaneous velocity-concentration measurements were carried out at stations in the recirculation zone at reattachment and downstream of reattachment. The axial inlet and bleed velocities were 70 m/s and 0.5 m/s, respectively. The latter corresponds to a typical gasification rate of the solid fuel in an SFRJ.

Vertical velocity profiles and turbulence intensities obtained from 10,000 data points per location for the seeded flow agreed reasonably well with those obtained from 1000 data points in the combined LDV-Rayleigh mode using dust as seeding. Thus, there is little loss in accuracy in the velocity measurements when restricting the number of data points to 1000. Similar comparisons were carried out between the concentration data measured continuously using 32,000 values per station and concentrations obtained from velocity-triggered measurements obtained from 1000 averaged values per location. These are shown in Fig. 1. Although there is somewhat more scatter in the data from the joint measurements than in those from the pure measurements, overall agreement is good and no bias toward air is indicated. None of the concentration pdf's were bimodal. Thus, the residence times of the bleed gases close to the porous plate zone were long enough for molecular mixing to prevent any pockets of bleed gas to be observed above 0.1 step heights above the bleed plate.

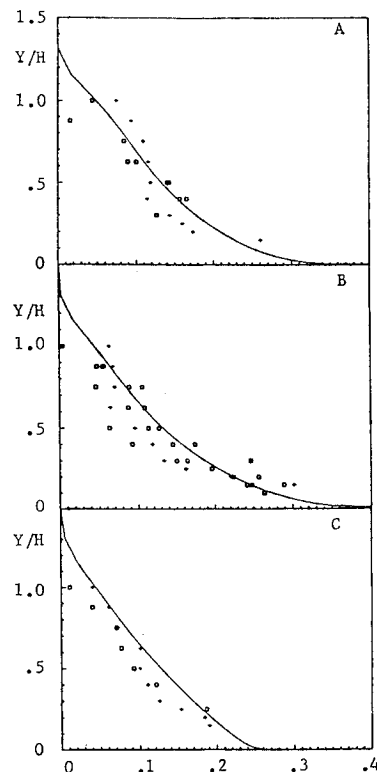


Fig. 1 Concentration of bleed gas vs height above the tunnel floor for CO_2 -air mixture as injectant gas at different axial locations: A-5.9 stepheights, B-7.3 stepheights, and C-8.8 stepheights; +, continuous data acquisition; o, seed particles triggered data acquisition; -, predicted using $k-\epsilon$.

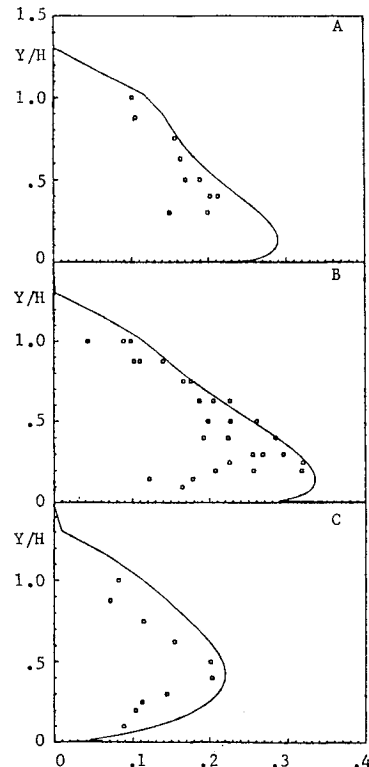


Fig. 2 Velocity bleed gas concentration correlation vs height above the tunnel floor for CO_2 -air mixture as injectant gas at different axial locations: A-5.9 stepheights, B-7.3 stepheights, and C-8.8 stepheights; o, seed particles triggered data acquisition; -, predicted using $k-\epsilon$.

Figure 1 shows representative samples of the concentration profiles at distances 5.9, 7.3 (reattachment), and 8.8 stepheights downstream of the step. Also shown are the profiles

calculated using the modified $k-\epsilon$ model.¹ The measurements clearly agree well with the predicted values. The concentration gradients generally were correctly predicted in the forward part of the recirculation zone and somewhat underpredicted past reattachment. Downstream of reattachment, the main and bleed gases, thus, were slightly better mixed than predicted. Closer to the step, the process was more diffusion-controlled. This observation is in close agreement with the expectations from the velocity measurements.¹ Furthermore, the mean concentration data obtained using the more sophisticated deconvolution are not significantly different from those obtained with the simple data reduction technique.²

The real power of this improved technique, however, becomes evident when calculating the velocity-concentration covariances, which could not be obtained at all using the simplified data reduction scheme. Figure 2 shows the profiles of the velocity-concentration covariances at the same locations in the test section as in the previous example. Once again, the predicted values are shown as a solid line. Clearly, the agreement between the measured and calculated values of the covariance is not as good as those for the mean concentrations. In part, this could be due to remaining uncertainties in the measured values of the covariance. However, Fig. 2b, which corresponds to the reattachment location, indicates acceptable reproducibility of the data, especially considering the low signal-to-noise ratio of the measurements. Therefore, it appears that whereas the model quite accurately predicts the overall shape of the covariance profiles, it consistently overpredicts the magnitude of the covariance.

Conclusions

Molecular mixing in the recirculation zone, behind a backward-facing step with bleed, was found to be excellent. Agreement between the measured bleed gas concentration profiles and those predicted using a modified $k-\epsilon$ model were very good, although the flow downstream of recirculation was found to be better mixed than predicted. An improved data reduction technique for removing background noise really showed its full potential in the extraction of the velocity-concentration covariance. Despite the remaining uncertainties in the covariance, it becomes clear that the $k-\epsilon$ model, while correctly calculating the shape of the profile, tends to overpredict the magnitude of the velocity-concentration covariance.

Acknowledgment

This work was supported by the Air Force Office of Scientific Research under Grant AFOSR-83-0356. The authors wish to thank Dr. W. C. Strahle for developing the data reduction technique and for his extensive contributions to this work. Thanks also to Dr. R. Latham for his help in coding the data acquisition software.

References

- ¹Richardson, J., de Groot, W. A., Jagoda, J. I., Walterick, R. E., Hubbart, J. E., and Strahle, W. C., *Journal of Propulsion and Power*, Vol. 1, No. 6, Nov.-Dec. 1985, pp. 488-493.
- ²de Groot, W. A., Latham, R., Jagoda, J. I., and Strahle, W. C., *AIAA Journal*, Vol. 25, Aug. 1987, pp. 1142-1144.
- ³Walterick, R. E., de Groot, W. A., Jagoda, J. I., and Strahle, W. C., AIAA Paper 88-0052, Jan. 1988.
- ⁴Penney, C. M., *Journal of the Optical Society of America*, Vol. 59, Jan. 1969, pp. 34-38.
- ⁵Driscoll, J. F., Schefer, R. W., and Dibble, R. W., "Mass Fluxes $\rho'u$ " and $\rho'v$ " Measured in a Turbulent Nonpremixed Flame," *Proceedings of the 19th International Symposium on Combustion*, The Combustion Inst., Pittsburgh, PA, 1982, pp. 477-485.
- ⁶Schefer, R. W. and Dibble, R. W., *AIAA Journal*, Vol. 23, July 1985, pp. 1070-1078.
- ⁷Strahle, W. C. and de Groot, W. A., "Extraction of Useful Data from Noise Contaminated PDF's," *Combustion and Flame* (to be published).

Diagonal Implicit Multigrid Calculation of Inlet Flowfields

D. A. Caughey* and R. K. Iyer†
Cornell University, Ithaca, New York

I. Introduction

A DIAGONAL implicit multigrid algorithm to solve the Euler equations has been applied by Caughey¹ to compute the transonic flow past a two-dimensional airfoil. It is the purpose of this Note to describe an extension of that algorithm to compute the supersonic flow past and within a two-dimensional planar inlet.

II. Analysis

Inviscid compressible flows are governed by the Euler equations, which are written in conservation form in order to capture shocks correctly. The integral form of the conservation laws is

$$\frac{\partial}{\partial t} \iint_S w \, dx \, dy + \int_{\partial S} (f \, dy - g \, dx) = 0 \quad (1)$$

where w is the vector of flow variables and f, g are the flux vectors in the x and y coordinate directions. The integration is over the region S with boundary ∂S . In the present discretization, which is based on that of Jameson et al.,² the temporal and spatial approximations are kept separate. This decoupling ensures a steady-state solution that is independent of the time step with which the solution is advanced from some initial condition. The spatial discretization is performed using a finite-volume approximation, which consists in applying the integral form of the conservation laws as defined by Eq. (1) to each quadrilateral cell in the physical domain. In the present calculation, the flow variables are taken to represent the average values for each mesh cell. The values required for the evaluation of the fluxes in Eq. (1) are taken to be constant on each face, and equal to the simple average of the values corresponding to the cells which share the face. This formulation is equivalent to a centered difference scheme that is second-order accurate in the mesh spacing in the physical domain when the mesh is smooth.

The use of centered differences has the drawback of allowing the solution to decouple at odd- and even-numbered points and of allowing oscillations in the solution near shock waves. To counter these effects, following Jameson et al.,² a blend of second- and fourth-difference artificial dissipation terms is added to the equations. The difference approximation, including dissipation terms, can be written in the form

$$\frac{dw_{i,j}}{dt} + Qw_{i,j} - Dw_{i,j} = 0 \quad (2)$$

where Q and D are, respectively, the operators representing the spatial discretization of the flux terms and the dissipative terms. The artificial dissipation is constructed such that simultaneously the second-difference terms are activated and the fourth-difference terms are switched off near shock waves, allowing them to be captured with little or no overshoot. The normalized second-difference of the pressure

$$v_{i,j} = \frac{|p_{i+1,j} - 2p_{i,j} + p_{i-1,j}|}{p_{i+1,j} + 2p_{i,j} + p_{i-1,j}}$$

is used to modulate these dissipative terms.

Received Feb. 29, 1988; revision received April 27, 1988. Copyright © American Institute of Aeronautics and Astronautics, Inc., 1988. All rights reserved.

*Professor, Sibley School of Mechanical and Aerospace Engineering, Associate Fellow AIAA.

†Graduate Research Assistant, Sibley School of Mechanical and Aerospace Engineering.